Indirect optical absorption and origin of the emission from -FeSi 2 nanoparticles: Bound exciton (0.809 eV) and band to acceptor impurity (0.795 eV) transitions

R. Lang, L. Amaral, and E. A. Meneses

Citation: Journal of Applied Physics **107**, 103508 (2010); doi: 10.1063/1.3391977
View online: http://dx.doi.org/10.1063/1.3391977
View Table of Contents: http://scitation.aip.org/content/aip/journal/jap/107/10?ver=pdfcov
Published by the AIP Publishing

Indirect optical absorption and origin of the emission from β-$FeSi_2$ nanoparticles: Bound exciton (0.809 eV) and band to acceptor impurity (0.795 eV) transitions

R. Lang,[1,a] L. Amaral,[1] and E. A. Meneses[2]
[1]*Programa de Pós-Graduação em Ciências dos Materiais (PGCIMAT, Instituto de Física, UFRGS, Porto Alegre, 15051/91501-970 Rio Grande do Sul, Brazil*
[2]*Instituto de Física Gleb Wataghin, UNICAMP, Campinas,13083-970 São Paulo, Brazil*

(Received 21 July 2009; accepted 15 March 2010; published online 20 May 2010)

We investigated the optical absorption of the fundamental band edge and the origin of the emission from β-$FeSi_2$ nanoparticles synthesized by ion-beam-induced epitaxial crystallization of Fe^+ implanted SiO_2/Si(100) followed by thermal annealing. From micro-Raman scattering and transmission electron microscopy measurements it was possible to attest the formation of strained β-$FeSi_2$ nanoparticles and its structural quality. The optical absorption near the fundamental gap edge of β-$FeSi_2$ nanoparticles evaluated by spectroscopic ellipsometry showed a step structure characteristic of an indirect fundamental gap material. Photoluminescence spectroscopy measurements at each synthesis stage revealed complex emissions in the 0.7–0.9 eV spectral region, with different intensities and morphologies strongly dependent on thermal treatment temperature. Spectral deconvolution into four transition lines at 0.795, 0.809, 0.851, and 0.873 eV was performed. We concluded that the emission at 0.795 eV may be related to a radiative direct transition from the direct conduction band to an acceptor level and that the emission at 0.809 eV derives from a recombination of an indirect bound exciton to this acceptor level of β-$FeSi_2$. Emissions 0.851 and 0.873 eV were confirmed to be typical dislocation-related photoluminescence centers in Si. From the energy balance we determined the fundamental indirect and direct band gap energies to be 0.856 and 0.867 eV, respectively. An illustrative energy band diagram derived from a proposed model to explain the possible transition processes involved is presented. © *2010 American Institute of Physics*. [doi:10.1063/1.3391977]

I. INTRODUCTION

Semiconducting silicides are of significant interest as a possible route to obtain novel silicon-based technologies in optoelectronics and optical interconnects.[1] Among the transition-metal silicides, semiconductor β-$FeSi_2$ has received considerable attention as a promising material for application in photodetectors,[2] solar cells,[3] and light emission devices,[4] due to its photoresponse properties in the near-infrared region at about 1.55 μm (Ref. 5) a relevant wavelength to optical communication.

In the last two decades, the nature of the band gap of this compound was a matter of debate, as well as the origin of the photoluminescence (PL) related to the radiative complex formation observed at ~ 0.8 eV, which is still questionable in some cases due to the concomitant presence of extended defects in the Si matrix. This is especially important when it involves synthesis by ion beam implantation. These defects show a few luminescence peaks (the well known lines D1–0.812 eV, D2–0.875 eV, D3–0.934 eV, and D4–1.000 eV)[6] in the same spectral range where the recombination emission from the silicide is expected to be.

Band structure calculations for β-$FeSi_2$ have indicated that there is a minimum indirect band gap (~ 0.8 eV) a few tens of milli-electron-volt below the direct band gap.[7] Moreover, this band gap has a high sensitiveness to lattice distortions and it is expected that the presence of suitable strain fields will make it possible to transform it into a direct one with a strong oscillator strength.[8,9] From this point of view, the study of the formation of isolated nanoparticles will be of interest to explore that prediction and additionally to complement low-dimensional structure knowledge for optoelectronic applications.

Previous experiments by Grimaldi *et al.*[10] and Martinelli *et al.*[11] showed that elastically strained ball-shaped particles (formed by ion-beam synthesis) surrounded by a defect-free matrix do not have luminescence properties, whereas unstrained disk-shaped particles in a matrix with a large number of defects emit around 0.805 eV. Absorbance measurements of the latter have suggested the existence of a direct band gap. Nevertheless, this result is incompatible with the PL structure they observed. A large number of the experimental results on optical properties of β-$FeSi_2$, available in the literature, are contradictory or vary considerably under the same synthesizing techniques, and do not provide a consistent picture of luminescence and fundamental gap determinations.

This work aims to explain the origin of the radiative transitions at 0.795 and 0.809 eV observed in the PL spectra at low temperatures of β-$FeSi_2$ nanoparticles synthesized by

[a]Author to whom correspondence should be addressed. Present address: Ion Implantation Laboratory–UFRGS Porto Alegre, RS, Brazil. Electronic mail: rlang@if.ufrgs.br.

an alternative method, ion implantation followed by ion-beam-induced epitaxial crystallization (IBIEC) and post-thermal annealing.

The goal is not only to demonstrate that these transitions come from this material, but also to explain and quantify the formation of complexes that originate the emission of photons with such energies. In the process we tested the band gap conversion-indirect to direct when the nanoparticles are under strain.[8,9]

In Sec. II we describe the experimental procedures. In Sec. III we present the obtained experimental results and an extensive analysis of them. Here, we come to the conclusion that the emission at 0.795 eV originates from the recombination of electrons in the direct conduction band with holes in an acceptor level, and that the emission at 0.809 eV derives from recombination of indirect bound exciton to the neutral acceptor mentioned above. We present here a schematic energy band diagram showing the possible transitions.

II. EXPERIMENTAL

We used an *n*-type Czochralski Si (001) wafer (thickness 500 μm, resistivity 10–20 Ω cm) covered with a 30 nm SiO_2 (thin film formed by dry-oxidation) as a starting material. It has been suggested that the SiO_2/Si interface could reduce considerably the nucleation barrier for β-$FeSi_2$.[12] To that purpose Fe^+ ions were implanted at cryogenic temperature ($\sim$ 90 K) in two steps with different implantation energies: (i) 70 keV at the fluence of 5×10^{15} cm^{-2} and (ii) 40 keV at the fluence of 3×10^{15} cm^{-2}, in order to produce broad ion distribution near the SiO_2/Si interface. The Rutherford backscattering spectrometry concentration-depth profile indicated a peak concentration of $\sim$ 3.5 at. % at 52 nm from the surface. Previous IBIEC experiments for an approximate peak concentration have determined the existence of a single γ-$FeSi_2$ cubic phase.[13] Subsequently, the Fe-implanted amorphous layer ($\approx$105 nm thickness) was recrystallized by high energy irradiation with Si^+ ions at 600 keV ($\Phi=6\times10^{16}$ cm^{-2}) with the target kept at 350 °C (IBIEC process - for a review of this method, see Ref. 14). After the induced recrystallization, some samples were thermally annealed in a gaseous atmosphere (95% N_2 –5% H_2:0.5 l/min) at temperatures between 700–900 °C to ensure complete phase transition and coarsening of the nanoparticles.

The formation and phase transition were identified through the micro-Raman scattering spectroscopy (μRSS) experiments, which also allowed us to obtain information about the microstructural quality and the strain state of the nanoparticles. The μRSS measurements were performed at room temperature using a JY-T64000 Raman system (three coupled 640 mm monochromators with 1800 grooves/mm holographic gratings). The spectra were obtained in a backscattering geometry with the polarization configuration $z(x,x)\bar{z}$, being $z\|[001]_{Si}$ and $x\|[100]_{Si}\rightarrow001(100,100)00\bar{1}$ (Porto's notation). This polarization configuration was chosen according to the Raman selection rules for Si in order to allow the signals from the synthesized material to be distinguished from those of the substrate. The Raman lines were excited by the 514.5 nm line of an Ar^+ ion laser. The average laser power on the sample surface was 5 mW and the spot diameter estimated as $\sim$ 0.8 μm. The scattered light was detected by a liquid nitrogen cooled charge-coupled device back illuminated detector, with a spectral resolution higher than 2 cm^{-1}, whereas the accuracy of the peak center was about $\pm$0.05 cm^{-1}. The accumulation time was 1200 s.

The β-$FeSi_2$ microstructure of the samples was observed and characterized by transmission electron microscopy (TEM) (JEOL 2010 operating at 200 kV). Plan-view and cross-sectional specimens were prepared using a combination of mechanical thinning (polished to $\sim$ 30 μm) and Ar^+ ion milling (the glancing angle of argon ions at 2.5 keV was as low as 4°).

The optical absorption near the fundamental gap edge of β-$FeSi_2$ nanoparticles was analyzed by spectroscopic ellipsometry (SE). Ellipsometry data were acquired with a variable-angle ellipsometer SOPRA GES-5E equipped with a high pressure Xe discharge lamp source, a rotating polarizer, an analysis polarizer (fixed) and a microspot accessory (numerical aperture of 3°) that focuses the light beam into a small region of the sample surface (365×270 μm^2). The near infrared ellipsometric measurements (1–1.7 μm spectral range with step of 0.004 μm) were made at an angle of incidence of 75° (best measurement sensitivity) at room temperature.

A PL spectroscopy detailed investigation at low temperatures was carried out in a continuous flow variable-temperature optical He cryostat. The same 514.5 nm line of Ar^+ ion laser used in micro-Raman measurements was employed as a photoexcitation source, with an estimated excitation power density of 45 mW/mm^2. The light emission was dispersed using a single-grating monochromator (SPEX 0.5 m focal length with 600 l/mm grating and 32 Å/mm resolution) and detected by a liquid-N_2 cooled Ge $p-i-n$ photodiode in the wavelength region of 1.1–1.8 μm. Standard lock-in technique was used to improve the signal to noise ratio. The PL spectra were corrected for the overall spectral response of the experimental set up.

III. RESULTS AND DISCUSSION

The Raman spectra in the wave number range between 170 and 270 cm^{-1} are shown in Fig. 1. The spectrum corresponding to the as-IBIEC sample does not show, as expected, any characteristic Raman peaks for the β-$FeSi_2$ phase. However, after annealing the sample at 700 °C/1 h, additional lines are observed at about 194 cm^{-1} ($\sim$ 24 meV) and 249 cm^{-1} ($\sim$ 31 meV) attributed to A_g-mode-related Raman active[15] and at about 177, 200, and 255 cm^{-1} assigned as contributions of the Raman active B_{1g} mode[16] of the β orthorhombic structure. We also observed the Raman intensity enhancement and line narrowing with increasing annealing temperature, which is caused by the volume increase of the β-$FeSi_2$ nanoparticles via the inhomogeneous Ostwald ripening process and by the crystallinity improvement of the material. As evidenced by the very narrow Raman lines, the sample annealed at 900 °C/7 h has an excellent crystalline quality. The full width at half maximum (FWHM) of the

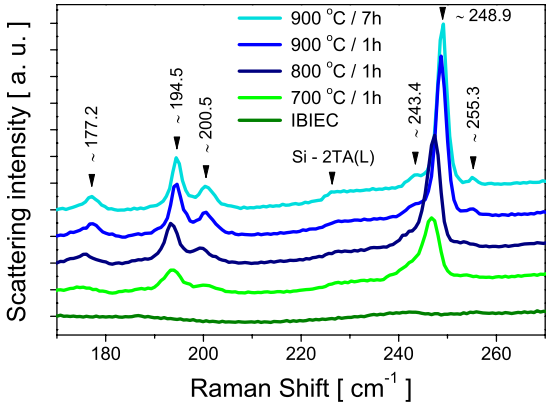

FIG. 1. (Color online) Micro-Raman scattering spectra of samples recrystallized by IBIEC process and subsequently annealed in a gaseous atmosphere at different temperatures and times. The prominent Raman lines at 194 and 249 cm^{-1} are features from active A_g modes of the orthorhombic β-$FeSi_2$ phase.

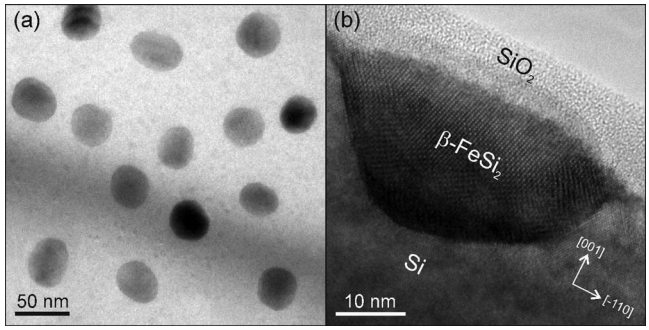

FIG. 2. Bright-field contrast TEM images of the 900 °C/7 h annealed sample. (a) Plan-view taken along the $[001]_{Si}$ pole, (b) high-resolution cross-section taken at nearly $[110]_{Si}$ zone axis.

249 cm^{-1} main peak is estimated as 2.3 cm^{-1}, which is comparable to the values reported for β-$FeSi_2$ bulk crystals.[17] The scattering (step) at $\sim$ 226 cm^{-1} comes from two-phonon scattering transverse acoustic at the critical point L of the Brillouin zone 2TA(L) of the Si substrate.[18] Furthermore, a shoulder at $\sim$ 243 cm^{-1} is better defined as the annealing temperature increases. This peak was also observed in other β-$FeSi_2$ samples reported previously produced by several methods,[19,20] but it has not been detected in β-$FeSi_2$ single crystals (even under different polarization configuration).[16,17] Hence, these observations suggest that the peak at 243.4 cm^{-1} as shown in Fig. 1 may be associated to disorder-induced Raman scattering related to Si vacancies at the matrix/nanoparticles interfacial region.[21]

The signal intensity at 248.9 cm^{-1} seems to saturate for samples thermally treated at 900 °C, indicating that annealing at 900 °C/1 h is sufficient to achieve complete transition from γ phase to β one. The TEM observations show that β-$FeSi_2$ nanoparticles are formed after thermal annealing and are localized at the SiO_2/Si interface within the Si matrix, without any preferential orientation. It was also noted that the increasing treatment temperature leads to an increase in the nanoparticle size, from 20 ± 3 nm (for the 700 °C/1 h treated sample) to 40 ± 4 nm diameter (after 900 °C treatment for 1 or 7 h) and, at the same time, leads to a decrease in the nanoparticle density, in agreement with Raman scattering results described above. The Fig. 2 exhibits representative bright-field TEM micrographs of the 900 °C/7 h annealed sample. The plan-view image, such as Fig. 2(a), taken along the $[001]_{Si}$ pole reveals that the isolated nanoparticles produced are dispersed into the substrate. The high-resolution cross-sectional image [Fig. 2(b)] taken at nearly $[110]_{Si}$ zone axis, shows in detail an β-$FeSi_2$ nanoparticle at the SiO_2/Si interface with a typical hemispherical-like structure, and according to the plan-view image the base (top view) of these nanoparticles are approximately circular or oval.

Moreover, slight Raman shift toward higher energies are observed for all the lines from iron disilicide [Fig. 1]. This blueshift can be related to stress effect. In general, for compressive strain, a decrease of the lattice parameter increases the frequency of the vibrational modes.[22] However, it is known that the increase of the annealing temperature leads to the nanoparticles+matrix system relaxation (elastic equilibrium). In our case, the detected blue shifts of the lines, which tend to the fully relaxed bulk mode, can be a consequence of the decreasing of the stress (in both nanoparticles and embedding matrix) after the treatment at higher temperatures. During the relaxation process, the stress/strain is mostly relieved by the generation of structural disorder (misfit dislocation, lattice mismatch, distorted bonds, etc.); certain types of defects are created in the host matrix while others are confined to the SiO_2/β-$FeSi_2$/Si interfaces. These defects, as will be mentioned later, might act as radiative recombination centers at low temperature. In summary, the μRSS and TEM characterization attests the formation of strained β-$FeSi_2$ nanoparticles and the structural quality of the synthesized material.

The optical absorption near the fundamental gap edge was evaluated by the optical parameter-extinction coefficient (k) obtained by SE. Due to the small amount of silicide present in the samples (low dose implantation), it was impossible to obtain reliable information about the nature of the band gap through conventional methods such as optical transmittance/reflectance measurements. In contrast, SE is a highly sensitive nondestructive technique and has been employed lately for optical characterization of nanocrystalline semiconductors materials-providing for surface information as desired in our study.[23] The real (n-refractive index) and imaginary (k-extinction coefficient) parts of complex refractive index ($N=n-ik$) were directly calculated from the measured ellipsometric angle Psi (ψ) and phase difference Delta (Δ) as a function of wavelength, by fitting of the modeled Psi and Delta spectra to the experimental spectra. The n and k values are obtained using the ellipsometer's analysis-modeling software, where the appropriate sample structure model SiO_2(30 nm)/$FeSi_2$(25 nm)/Si(bulk) is utilized. The analysis-modeling software assumes an isotropic medium and a homogeneous behavior. With this procedure, the extinction coefficient obtained represents a mixture of the extinction coefficients of the constituents of the adjacent regions. Hence, the photon energy dependent optical-absorption coefficient $\alpha(h\nu)$, of the sample as a whole, can be obtained by the following expression:

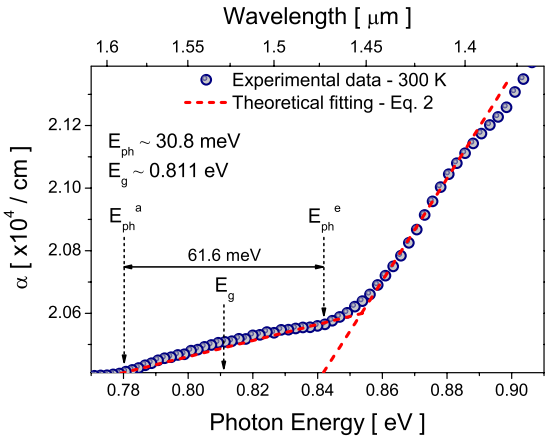

FIG. 3. (Color online) Room temperature optical absorption coefficient (α) vs photon energy ($h\nu$) from sample annealed at 900 °C/7 h. The dashed lines represent theoretical fitting by Eq. (2) assuming E_{ph}=30.8 meV as the energy of one phonon.

$$\alpha(h\nu) = 4\pi\frac{k(h\nu)}{\lambda}. \tag{1}$$

Figure 3 shows the spectral dependence of the optical absorption coefficient at room temperature of the sample annealed at 900 °C for 7 h, specifically in the energy range between 0.77 and 0.91 eV (edge-absorption). As shown in Fig. 3, the optical absorption coefficient magnitude is as high as 10^4 cm^{-1} around 0.8 eV, a typical value of α found for β-$FeSi_2$.[24] The spectrum on the low energy side suggests a step behavior (with phonons), characteristic of an indirect fundamental gap material.[25] In this figure, the points corresponding to E_{ph}^{a} (absorption, 0.7802 eV) and E_{ph}^{e} (emission, 0.8418 eV) refer to the thresholds of the step of phonon-assisted indirect transition. Their energy difference, 61.6 meV represents exactly two phonons replicas with energies equal to 0.0308 eV, which has also been identified as active by micro-Raman experiments (the highest-intensity peak, see Fig. 1). This phonon energy value is very close to other experimentally measured phonons at 31 (Ref. 25) and 30 meV.[26] A theoretical calculated value for this energy was estimated to be 35 meV.[27]

We have adjusted theoretical curves to the experimental data (in a process similar to the one used by Udono)[25] through the following approximate expression for optical absorption, assuming indirect allowed optical transition:[28]

$$\alpha(h\nu) = \frac{A(h\nu - E_g + E_{ph})^2}{\exp\left(\frac{E_{ph}}{k_B T}\right) - 1} + \frac{B(h\nu - E_g - E_{ph})^2}{1 - \exp\left(-\frac{E_{ph}}{k_B T}\right)}, \tag{2}$$

where E_{ph} is the phonon energy involved, and E_g is the band-gap energy. The quantities A and B are parameters containing the density-of-state effective masses of electrons and holes, and k_B is Boltzmann's constant. Considering only one phonon energy (E_{ph}=30.8 meV) in Eq. (2), we obtained the value of 0.811 eV for the indirect fundamental gap energy from the best fitting result (represented by dashed curves in Fig. 3). The ellipsometry optical data do not show a renormalized band gap for the β-$FeSi_2$ nanoparticles, but only an indirect band gap. In addition, all Raman scattering lines

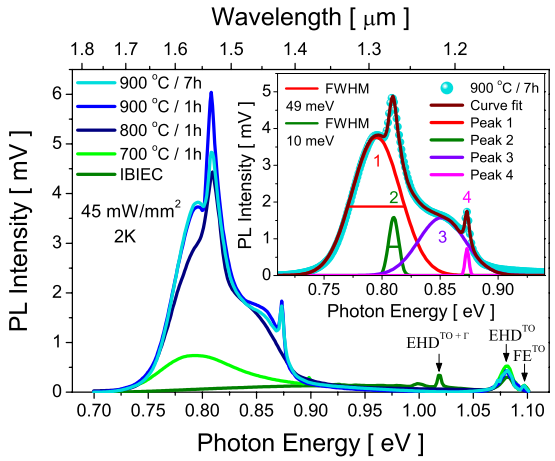

FIG. 4. (Color online) Photoluminescence evolution of the thermally treated samples after the IBIEC process. The PL was excited by an Ar^+ ion laser with a 514.5 nm line (~ 45 mW/mm^2) and measured at 2 K. The inset shows the deconvolution of the PL spectrum (for the sample annealed at 900 °C/7 h, circles) into four peaks. The solid lines show the fit results.

from nanoparticles (for this sample 900 °C/7 h) are comparable to β-$FeSi_2$ bulk crystals[17] and polycrystalline films[19] regarding both intensity and energy position. Therefore, taking into consideration the optical properties observed for the β-$FeSi_2$ nanoparticles under both aforementioned experiments we will consider the system under study behaving like crystalline particles.

Figure 4 shows the PL spectra taken at 2 K for each synthesis stage. As can be noticed, the evolution of PL emission spectra is accompanied by the formation process of the β-$FeSi_2$ phase. In accordance with the information obtained by μRSS measurements, the stabilization and complete coarsening of the material occur with thermal treatments at 900 °C. No detectable PL signal was found for the as-implanted sample. A likely reason for the absence of luminescence in this sample is the high density of nonradiative recombination centers produced by the generation of point defects in the course of implantation (amorphization). The as-IBIEC sample presented no significant PL emission; just a very weak peak at 1.00 eV coinciding with the energy of the D4 line (defects-related) and three excitonic complex emissions from Si substrate. These are indicated in Fig. 4 by electron-hole droplet $EHD^{TO+\Gamma}$ (1.019 eV), EHD^{TO} (1.081 eV), and free exciton FE^{TO} (1.096 eV).[6]

After thermal treatment at 700 °C/1 h, a broad band appears centered at ~ 0.79 eV. Annealing at 800 °C/1 h, however, causes a dramatic change in the intensity and in the morphology of the PL. An intense emission at ~ 0.81 eV superimposed by a broad shoulder centered at ~ 0.85 eV is detected. Furthermore, it is also observed the evolution of a band at ~ 0.79 eV, which contributes enormously to the spectrum. Upon annealing at higher temperature, such as 900 °C/1 h, the peak (~ 0.81 eV) reaches a maximum intensity, and a new narrow line at ~ 0.87 eV is defined. For the annealings at 900 °C for 1h and at 900 °C for 7h, the line-shapes of the emissions and the most intense peak energy position (at ~ 0.8 eV) are similar and comparable to those observed in polycrystalline β-$FeSi_2$ films.[29,30] We did not observe any evidence of quantum-confinement effects in

the nanoparticles. This effect has been observed for this kind of material when the crystal size is smaller than the exciton Bohr radius of β-$FeSi_2$, a_B (5–6 nm).[31]

In order to make a more meaningful distinction, and in seeking to define and interpret the intrinsic lines from the β-$FeSi_2$ nanoparticles, we considered for analytical purposes the annealed sample at 900 °C for 7 h (from now on called S1). The inset of Fig. 4 shows a spectral deconvolution of the PL spectrum performed for the S1 sample. Gaussian fitting has determined four well defined emissions centered at 0.795 eV peak 1, at 0.809 eV peak 2, at 0.851 eV peak 3, and at 0.873 eV peak 4. It shall be mentioned that the energy positions of peaks 2 and 4 coincide exactly with the dislocation-related PL peaks D1 and D2, respectively. However, there is a relative consensus among some authors that, in specific configurations, emissions observed around 0.8 eV are attributed to optical radiative transitions in the semiconducting β-$FeSi_2$.[32,33]

For the reasons abovementioned we want to explore the soundness of the statement that peak 2 originates from the recombination of β-$FeSi_2$, and additionally show that the new line peak 1 is also an intrinsic emission, derived from the same material. In order to accomplish this, we have undertaken comparative PL experiments using nickel disilicide to disentangle the β-$FeSi_2$ intrinsic luminescence and D1 defects contribution. A new set of samples was synthesized in the same conditions (implantation/IBIEC/annealing) of the Fe samples, except that the Fe ions were exchanged by Ni ions. For comparative analysis, Fig. 5(a) shows two PL spectra (taken at 2 K) from Fe and Ni containing samples which were thermally treated at 700 °C for 1 h.

One observes that the PL spectra of these two samples are significantly different. First of all, the detected luminescence from Ni containing sample is fundamentally originated from radiative recombination of carriers at defects in the Si matrix (the broad band around 0.85 eV and the narrow peak at 0.9 eV which is attributed to a transition involving a radiation-damage-produced center).[34] The introduction of Ni in the Si substrate does not result in a semiconducting phase. In contrast, the Fe-implanted sample presents a prominent band at 0.795 eV, besides the contributions already observed in the Ni containing sample. Figure 5(b) shows the S1 and Ni containing samples emission spectra which were synthesized under equivalent conditions. Comparing them, we can see that the band at 0.795 eV of the S1 sample disappears in the Ni-implanted sample spectrum, while the emissions associated to typical dislocations in Si, including the D1 active defect around 0.8 eV whose intensity and linewidth (~ 2.3 mV; ~ 21 meV) differ from the emission at 0.809 eV of sample S1 (~ 4.8 mV; ~ 10 meV) remain in both samples. These differences both in intensity and linewidth suggest that the transition 0.809 eV originates from the β-$FeSi_2$ nanoparticles, and that the D1 defect contributes to the overall 0.809 eV emission observed from the S1 sample. In Ref. 33, this matter was studied through the implantation of other elements, with the purpose of distinguishing the intrinsic β-$FeSi_2$ PL from the extrinsic Si-substrate PL. As to the 0.795 eV emission, Figs. 5(a) and 5(b) clearly demonstrate that it emerges only from Fe-implanted samples, thus also originating from an optical radiative transition intrinsic to the silicide.

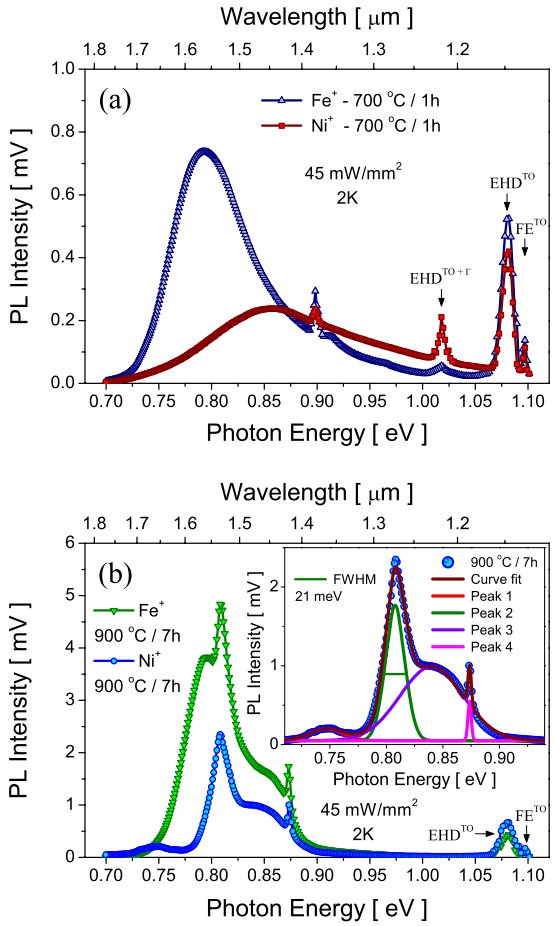

FIG. 5. (Color online) Comparative PL spectra of Fe and Ni samples synthesized in the same conditions (implantation/IBIEC/annealing). (a) Samples annealed at 700 °C/1 h and (b) samples annealed at 900 °C/7 h.

In what follows, we will explain the origin of the complex formation mechanism which results in the above emissions as we understand it. Reporting to the inset of Fig. 4, the FWHM of the lines 0.795 eV and 0.809 eV are 49 meV and 10 meV, respectively. These values show that the formation processes of the involved complexes are different. The band at 0.795 eV has a broad distribution, with a short lifetime possibly in the nanosecond range, while the band at 0.809 eV has a much more localized energy and a long lifetime possibly on the order of microseconds. Recombination processes of these transitions involve in the first case, band-to-band or band to impurity band, and in the second case, an excitonic process. In order to discuss the recombination processes, we show in Fig. 6 the variation of PL with temperature, between 10 and 130 K for S1 sample. Figure 6 shows that as the temperature increases, the PL associated to exciton process (0.809 eV) decreases in intensity, in relation to the alleged band-to-band transition or impurity-band transition (0.795 eV). This trend suggests that at higher temperatures, the complex involved will ionize and the spectrum will display only a PL around 0.795 eV or around 0.747 eV at room temperature. These energy values correspond to the same transition at 2 K and 300 K, respectively. Both are lower than

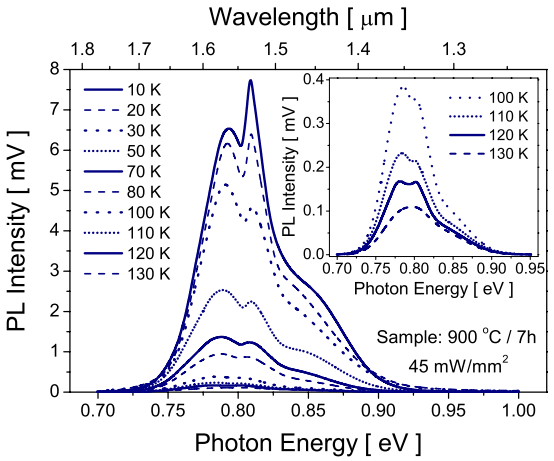

FIG. 6. (Color online) Temperature dependence of the PL intensity of the sample annealed at 900 °C for 7h. The spectra were acquired in the range T=10–130 K, with an estimated excitation power density of 45 mW/mm^2. The inset displays the behavior of thermal quenching above 100 K.

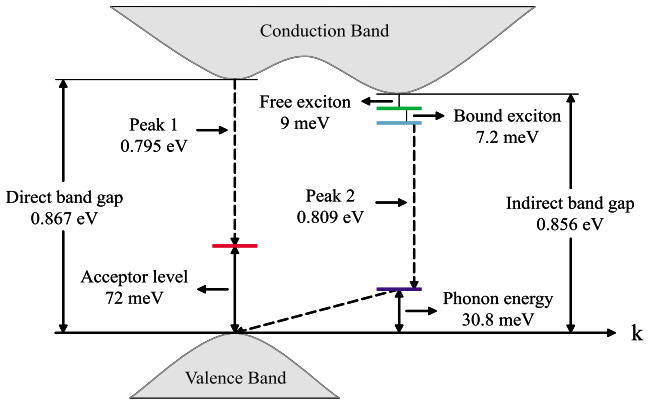

FIG. 7. (Color online) Schematic illustration of energy band structure for the indirect and direct fundamental gaps and the possible transition processes involved in β-$FeSi_2$ nanoparticles. Further details of the transitions are provided in the text.

the indirect fundamental energy gap at 300 K (0.811 eV) hence characterizing a transition from the conduction band to an acceptor impurity level. An acceptor level in β-$FeSi_2$ is reported by several authors.[35,36] Quantitative details of the energy balance will follow after the interpretation of the excitonic transition 0.809 eV (2 K). The transition at 0.809 eV, as mentioned above, has a linewidth of 10 meV (2 K) and, as we have seen in Fig. 6, this line practically disappears at 130 K (k_BT=11 meV), due to the ionization of the involved quasiparticles with the increase of the temperature. Therefore, we believe that this transition at 0.809 eV is the result of the recombination of a bound exciton to a neutral acceptor level.

In order to quantitatively demonstrate the complex formation mechanism, we carried out a temperature correction for the indirect fundamental gap (0.811 eV obtained by ellipsometry). Through the analysis of the experimental dependence of the peak energy 0.809 eV as a function of the temperature, and using the semiempirical Varshni relation,[37] we determined the value of the indirect gap energy to be E_g =0.856 eV, at 2 K. The binding energy of the bound exciton to the neutral acceptor E_{BE} can be calculated by the following expression:

$$E_{BE(binding)} = E_g - E_{FE} - E_{BE(transition)} - E_{ph} = 7.2 \text{ meV}, \quad (3)$$

where, E_g=0.856 eV is the fundamental indirect band gap energy, E_{FE}=9 meV is the free exciton binding energy (of the bulk β-$FeSi_2$ single crystal, in according to Ref. 38), E_{BE}=0.809 eV is the transition associated to this model and E_{ph}=30.8 meV is the phonon energy involved in the indirect transition - as estimated from data of Fig. 3. Using the expression of Haynes[39] for the binding energy of bound exciton to a neutral acceptor level E_A, we obtain

$$E_{BE(binding)} = 0.1E_A \Rightarrow E_A = 72 \text{ meV}. \quad (4)$$

This E_A value is comparable to those reported for the activation energy of the deep acceptor level in β-$FeSi_2$.[40,41] Thus, the 0.795 eV transition corresponds to a recombination of an electron in the conduction band to a hole in the deep acceptor level, with binding energy of 72 meV on top of the valence band. Therefore, the 0.795 eV corresponds to a direct transition, being the direct fundamental gap given by

$$E_g^{direct} = 0.795 \text{ eV} + 0.072 \text{ eV} = 0.867 \text{ eV}, \quad (5)$$

which is in good agreement with previous results.[11,42] The difference between direct and indirect band gap energies is 11 meV for the average of our β-$FeSi_2$ nanoparticles. Christensen[7] reported in a theoretical calculation (for a defect-free system/fully relaxed) an energy difference of approximately 35 meV (at T=0 K) between the indirect gap and the first direct transition. This prediction has been supported by some other experimental results which showed the existence of an indirect band gap only a few milli-electron-volt below a direct gap.[43] Figure 7 is a schematic energy band diagram for the indirect and direct fundamental gaps and the transition processes involved, constructed by utilizing the experimental energy measurements (0.809 and 0.795 eV) and the quantification resulted when using the proposed model. This estimated quasidirect band gap can be explained by the excellent crystalline quality of the nanoparticles and by the presence of slight strains derived from lattice distortion effects such as lattice mismatch between β-$FeSi_2$ and Si matrix during the growth via thermal annealing which were detected by stress effect (μRSS experiments).

IV. CONCLUSION

An illustrative energy band diagram derived from a proposed model to explain the possible transition processes involved in β-$FeSi_2$ nanoparticles embedded in SiO_2/Si substrate was presented. Explanations concerning the nature of emissions observed for the β-$FeSi_2$ nanoparticles (synthesized by ion implantation followed by IBIEC and post-thermal annealing) were possible by the analysis of measurements obtained utilizing several spectroscopic optical techniques. The results were as follows: we concluded that the transition at 0.795 eV might be an emission from β-$FeSi_2$ nanoparticles as a result of the direct recombination of electrons from a conduction band to holes in an acceptor impurity band. We confirmed that the 0.809 eV transition is also intrinsic to the β-$FeSi_2$ nanoparticles and might be associated

to the recombination of indirect bound exciton to the neutral acceptor whose binding energy is about 72 meV relative to the valence band top. Emissions at 0.851 and at 0.873 eV were assigned to be typical dislocation-related PL centers in Si. From the energy balance we determined the fundamental indirect band gap to be 0.856 eV and the direct band gap to be 0.867 eV. The small estimated difference (11 meV) between the band gaps is probably due to both the excellent crystalline quality of the β-$FeSi_2$ nanoparticles and the lattice distortions between iron disilicide and silicon that were compensated by strain in the silicide, which led the gap to become quasidirect.

ACKNOWLEDGMENTS

The authors would like to thank Professor F. Iikawa for his interest and help on the PL and micro-Raman measurements and also to thank Professor E. C. C. Vasconcellos for valuable suggestions in the manuscript. This work was partially supported by the Brazilian financial agencies CNPq and CAPES.

[1]V. E. Borisenko, *Semiconducting Silicides* (Springer, New York, 2000).
[2]K. Lefki and P. Muret, J. Appl. Phys. **74**, 1138 (1993).
[3]M. Powalla and K. Herz, Appl. Surf. Sci. **65–66**, 482 (1993).
[4]D. N. Leong, M. A. Harry, K. J. Reeson, and K. P. Homewood, Nature (London) **387**, 686 (1997).
[5]M. C. Bost and J. E. Mahan, J. Appl. Phys. **58**, 2696 (1985).
[6]R. Sauer, J. Weber, J. Stolz, E. R. Weber, K. H. Küsters, and H. Alexander, Appl. Phys. A: Mater. Sci. Process. **36**, 1 (1985).
[7]N. E. Christensen, Phys. Rev. B **42**, 7148 (1990).
[8]S. J. Clark, H. M. Al-Allak, S. Brand, and R. A. Abram, Phys. Rev. B **58**, 10389 (1998).
[9]L. Miglio, V. Meregalli, and O. Jepsen, Appl. Phys. Lett. **75**, 385 (1999).
[10]M. G. Grimaldi, C. Bongiorno, C. Spinella, E. Grilli, L. Martinelli, M. Gemelli, D. B. Migas, L. Miglio, and M. Fanciulli, Phys. Rev. B **66**, 085319 (2002).
[11]L. Martinelli, E. Grilli, D. B. Migas, L. Miglio, F. Marabelli, C. Soci, M. Geddo, M. G. Grimaldi, and C. Spinella, Phys. Rev. B **66**, 085320 (2002).
[12]J. Wong-Leung, D. J. Eaglesham, J. Sapjeta, D. C. Jacobson, J. M. Poate, and J. S. Williams, J. Appl. Phys. **83**, 580 (1998).
[13]R. L. Maltez, L. Amaral, M. Behar, A. Vantomme, G. Langouche, and X. W. Lin, Phys. Rev. B **54**, 11659 (1996) and references therein.
[14]F. Priolo and E. Rimini, Mater. Sci. Rep. **5**, 319 (1990).
[15]K. Lefki, P. Muret, E. Bustarret, N. Boutarek, R. Madar, J. Chevrier, J. Derrien, and M. Brunel, Solid State Commun. **80**, 791 (1991).
[16]H. Kakemoto, Y. Makita, Y. Kino, S. Sakuragi, and T. Tsukamoto, Thin Solid Films **381**, 251 (2001).
[17]Y. Maeda, H. Udono, and Y. Terai, Thin Solid Films **461**, 165 (2004).
[18]P. A. Temple and C. E. Hathaway, Phys. Rev. B **7**, 3685 (1973).
[19]Y. Maeda, K. Umezawa, Y. Hayashi, and K. Miyake, Thin Solid Films **381**, 219 (2001).
[20]R. Kuroda, Z. Liu, Y. Fukuzawa, Y. Suzuki, M. Osamura, S. Wang, N. Otogawa, T. Ootsuka, T. Mise, Y. Hoshino, Y. Nakayama, H. Tanoue, and Y. Makita, Thin Solid Films **461**, 34 (2004).
[21]F. Li, N. Lustig, P. Klosowski, and J. S. Lannin, Phys. Rev. B **41**, 10210 (1990).
[22]I. De Wolf, Semicond. Sci. Technol. **11**, 139 (1996).
[23]D. Barba, C. Dahmoune, F. Martin, and G. G. Ross, J. Appl. Phys. **105**, 013521 (2009).
[24]Z. Yang, K. P. Homewood, M. S. Finney, M. A. Harry, and K. J. Reeson, J. Appl. Phys. **78**, 1958 (1995); V. Darakchieva, M. Baleva, M. Surtchev, and E. Goranova, Phys. Rev. B **62**, 13057 (2000).
[25]H. Udono, I. Kikuma, T. Okuno, Y. Masumoto, and H. Tajima, Appl. Phys. Lett. **85**, 1937 (2004).
[26]K. Takakura, N. Hiroi, T. Suemasu, S. F. Chichibu, and F. Hasegawa, Appl. Phys. Lett. **80**, 556 (2002).
[27]A. B. Filonov, D. B. Migas, V. L. Shaposhnikov, N. N. Dorozhkin, G. V. Petrov, V. E. Borisenko, W. Henrion, and H. Lange, J. Appl. Phys. **79**, 7708 (1996).
[28]J. I. Pankove, *Optical Process in Semiconductors* (Dover, New York, 1971).
[29]H. Katsumata, Y. Makita, N. Kobayashi, H. Shibata, M. Hasegawa, and S. Uekusa, Jpn. J. Appl. Phys., Part 1 **36**, 2802 (1997).
[30]K. Yamaguchi, K. Shimura, H. Udono, M. Sasase, H. Yamamoto, S. Shamoto, and K. Hojou, Thin Solid Films **508**, 367 (2006).
[31]Y. Nakamura, R. Suzuki, M. Umeno, S. Cho, N. Tanaka, and M. Ichikawa, Appl. Phys. Lett. **89**, 123104 (2006).
[32]D. N. Leong, M. A. Harry, K. J. Reeson, and K. P. Homewood, Appl. Phys. Lett. **68**, 1649 (1996).
[33]Y. Maeda, Appl. Surf. Sci. **254**, 6242 (2008).
[34]G. Davies, Phys. Rep. **176**, 83 (1989).
[35]E. Arushanov, C. Kloc, and E. Bucher, Phys. Rev. B **50**, 2653 (1994).
[36]A. G. Birdwell, S. Collins, R. Glosser, D. N. Leong, and K. P. Homewood, J. Appl. Phys. **91**, 1219 (2002).
[37]Y. P. Varshni, Physica **34**, 149 (1967).
[38]A. G. Birdwell, T. J. Shaffner, D. Chandler-Horowitz, G. H. Buh, M. Rebien, W. Henrion, P. Staub, G. Behr, L. Malikova, F. H. Pollak, C. L. Littler, R. Glosser, and S. Collins, J. Appl. Phys. **95**, 2441 (2004).
[39]J. R. Haynes, Phys. Rev. Lett. **4**, 361 (1960) and references therein.
[40]C. Kloc, E. Arushanov, M. Wendel, H. Hohl, U. Malang, and E. Bucher, J. Alloys Compd. **219**, 93 (1995).
[41]K. Takakura, T. Suemasu, and F. Hasegawa, Jpn. J. Appl. Phys., Part 2 **40**, L249 (2001).
[42]H. Katsumata, Y. Makita, N. Kobayashi, H. Shibata, M. Hasegawa, I. Aksenov, S. Kimura, A. Obara, and S. Uekusa, J. Appl. Phys. **80**, 5955 (1996).
[43]C. Giannini, S. Lagomarsino, F. Scarinci, and P. Castrucci, Phys. Rev. B **45**, 8822 (1992).